NATIONAL HIGH MAGNETIC FIELD LABORATORY

Particle Reinforced Cu Matrix Conductors for High Field Magnets

FLORIDA STATE UNIVERSITY

Los Alamos NATIONAL LABORATORY

UF UNIVERSITY of FLORIDA

NATIONAL HIGH MAGNETIC FIELD LABORATORY

K.Han, R. E. Goddard, V. Toplosky, R.M. Niu, J. Lu, R. Walsh and D. N. Nguyen

FLORIDA STATE UNIVERSITY

Los Alamos NATIONAL LABORATORY

UF UNIVERSITY of FLORIDA

Abstract

The high strength conductors used in pulsed magnets in the US National High Magnetic Field Laboratory are manufactured from Cu matrix composites. One of the composites is made from particle reinforced Cu. The fabrication of these composite conductors requires high deformation strain, which creates high densities of dislocations and reduced particle spacing. Both mechanical strength and electrical conductivity can be predicted from particle spacing and dislocation density. When dislocation density reaches a certain value, the particle size, distribution and shape becomes important to mechanical properties. We studied the particle size, distribution and shape in high-strength conductors with respect to the properties of the conductors. The two most important factors related to above parameters were dislocations near the interface between the particle and the matrix, and the stress concentration near the particles. By engineering these variations, the properties of the conductors can be optimized. This paper reports our understanding of the relationship between critical properties and particle distribution in composite conductors for high field pulsed magnets.


Cu Cladding
Cu+alumina
EHT = 10.00 kV
WD = 5.2 mm
Mag = 3.60 K X
Signal A = InLens
Zeiss 1540 EsB
Date :3 Mar 2014
Time :10:26:17
2 µm

Fig. 1. SEM cross-section image taken by an in-lens detector showing microstructure of as-received GlidCop. Sample was cleaned by ion-beam to reveal the Cu grains. Cu cladding is at the upper left area and Cu+ alumina is at the lower right area. The image shows the size variation of the alumina particles.

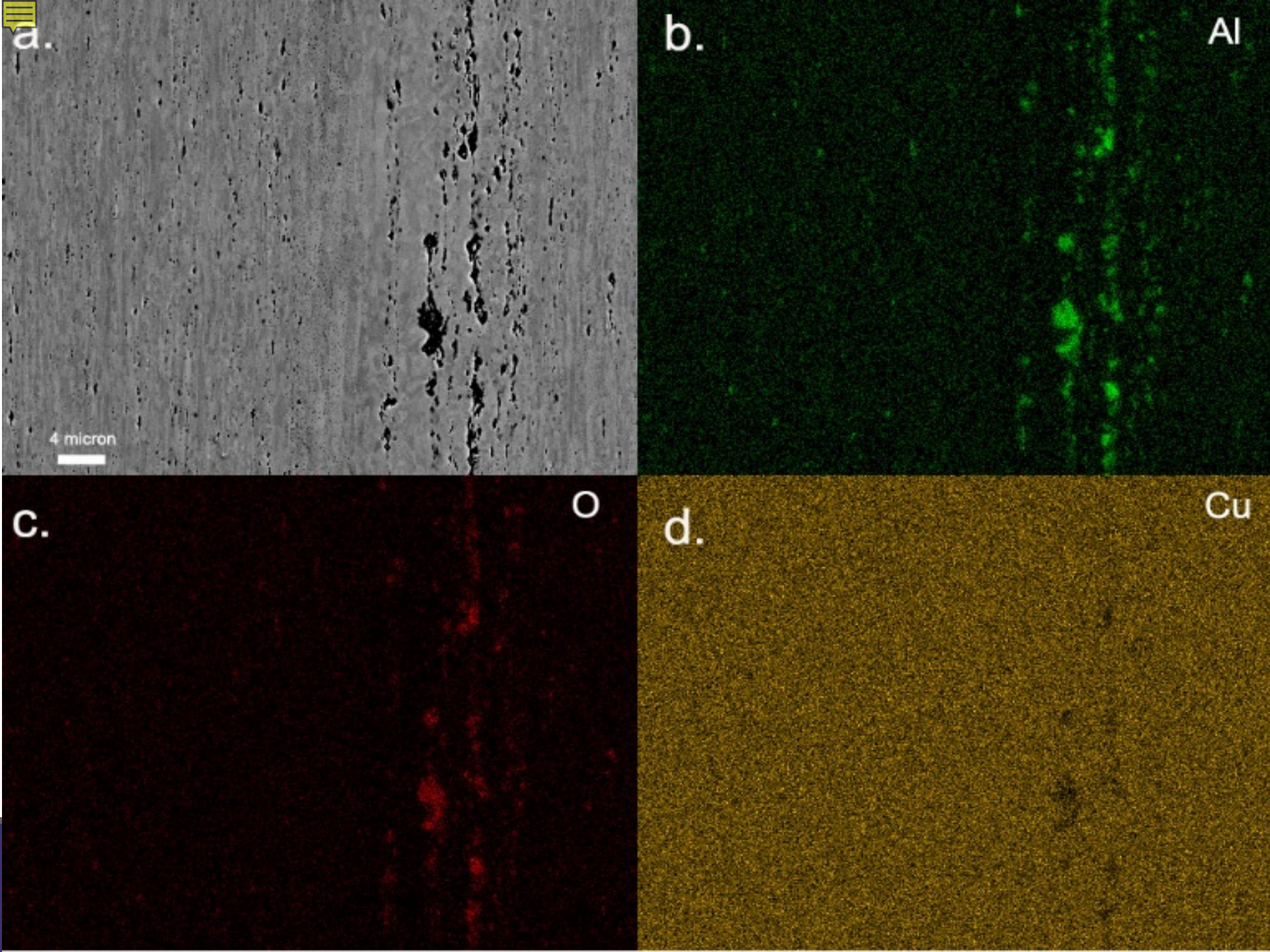
a.
4 micron
b.
Al
c.
O
d.
Cu

Fig. 2. SEM longitudinal cross-section image and EDX mapping of Cu+ alumina.

(a) SEM image taken by backscattered detector; (b) Aluminum mapping; (c) Oxygen mapping; (d) Copper mapping. The dark clusters in Fig. (a) correspond to areas rich in both aluminum and oxygen, indicating the presence of alumina. In the imaged area, the minimum alumina size is about 5 nm and the maximum reaches 5 μm. The image also shows that the alumina is not distributed homogeneously. Larger particles are mainly found in the right-hand of each imaged area.

TABLE I
MECHANICAL PROPERTIES OF AS-RECEIVED GLIDCOP AL15

Sample	Test Temperature	E (GPa)	YS (MPa)	TS (MPa)	Ef (%)	RA (%)
As-received	RT	90±4	302±9	378±1	46±1	80±1
As-drawn	RT	101±3	467±20	497±14	13±2	42±6
As-drawn	77 K	108±6	569±22	623±18	20±2	43±4

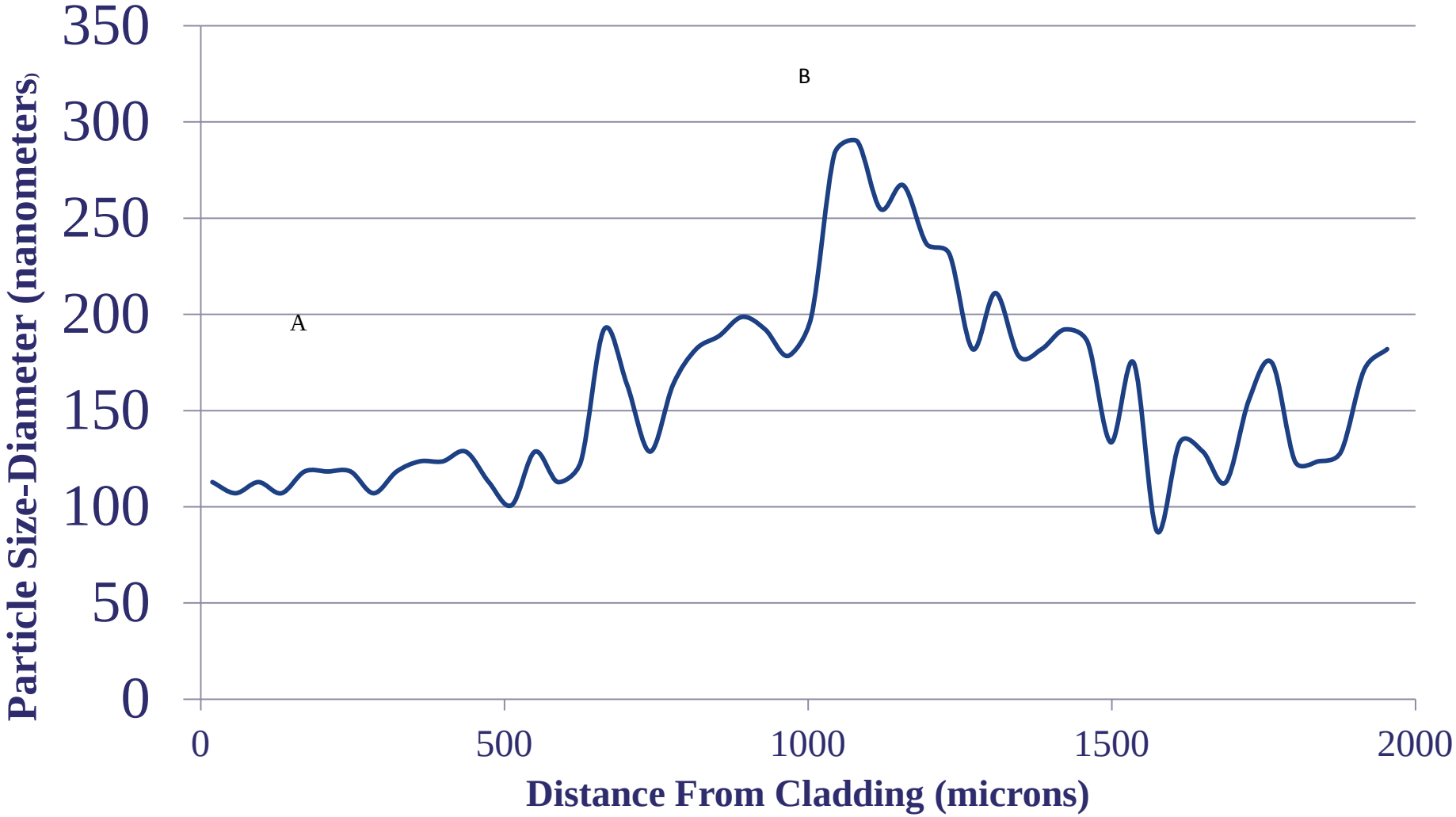
Particle Size-Diameter (nanometers)
350
300
250
200
150
100
50
0
0
500
1000
1500
2000
Distance From Cladding (microns)
A
B

Fig. 3a

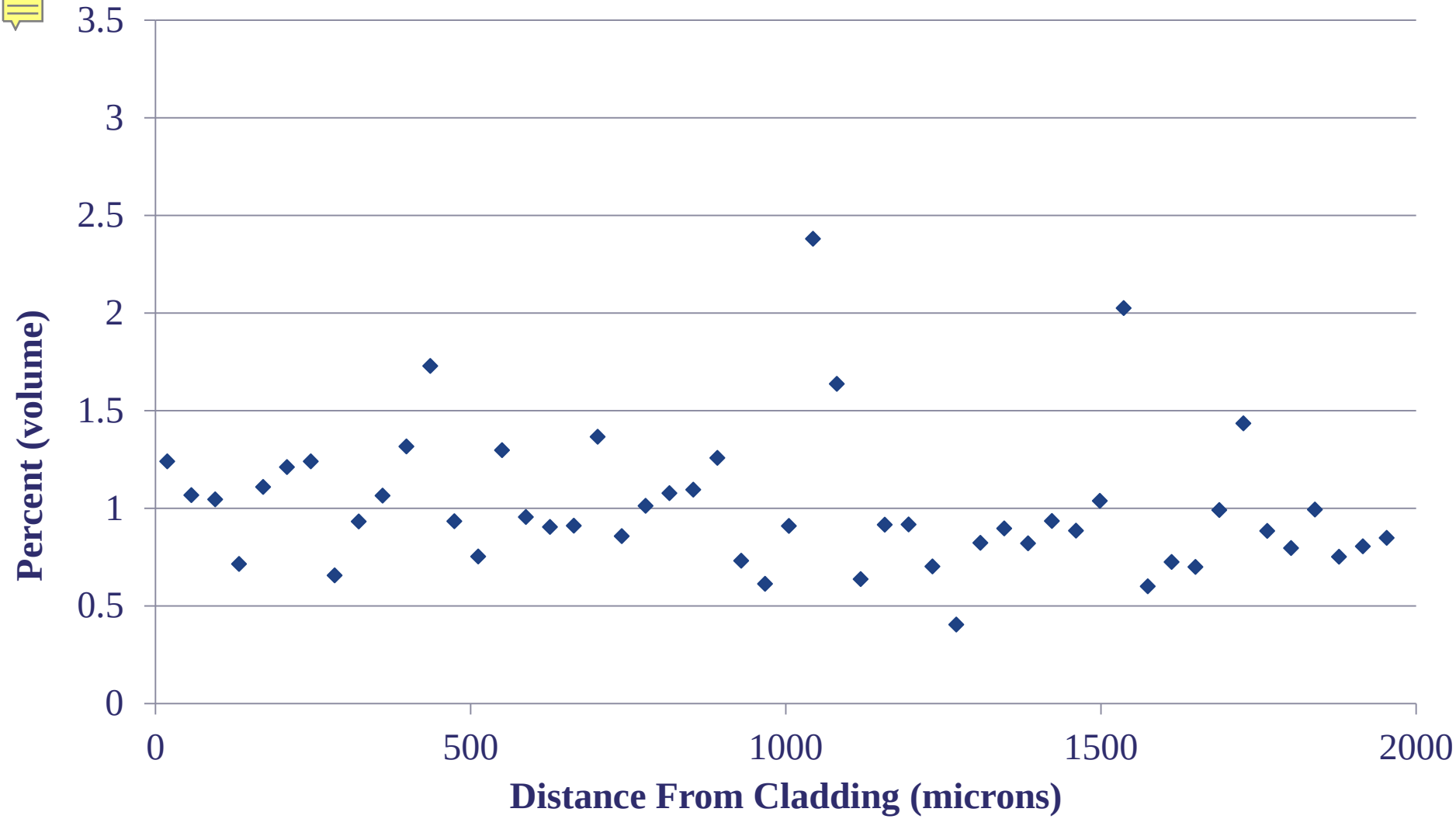
3.5
3
2.5
2
1.5
1
0.5
0
Percent (volume)
0
500
1000
1500
2000
Distance From Cladding (microns)

Fig. 3b

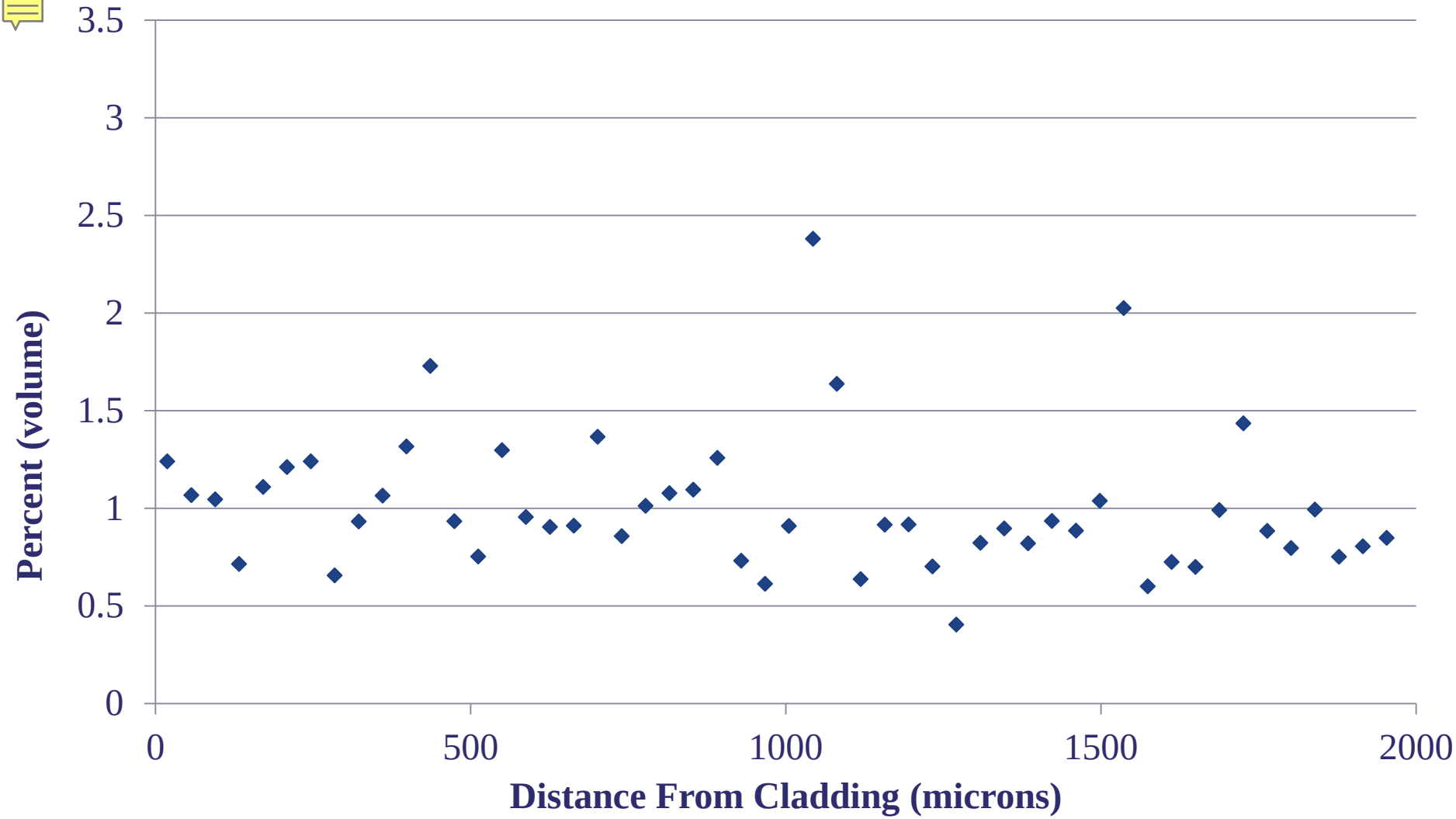
3.5
3
2.5
2
1.5
1
0.5
0
Percent (volume)
0
500
1000
1500
2000
Distance From Cladding (microns)

Fig. 3b

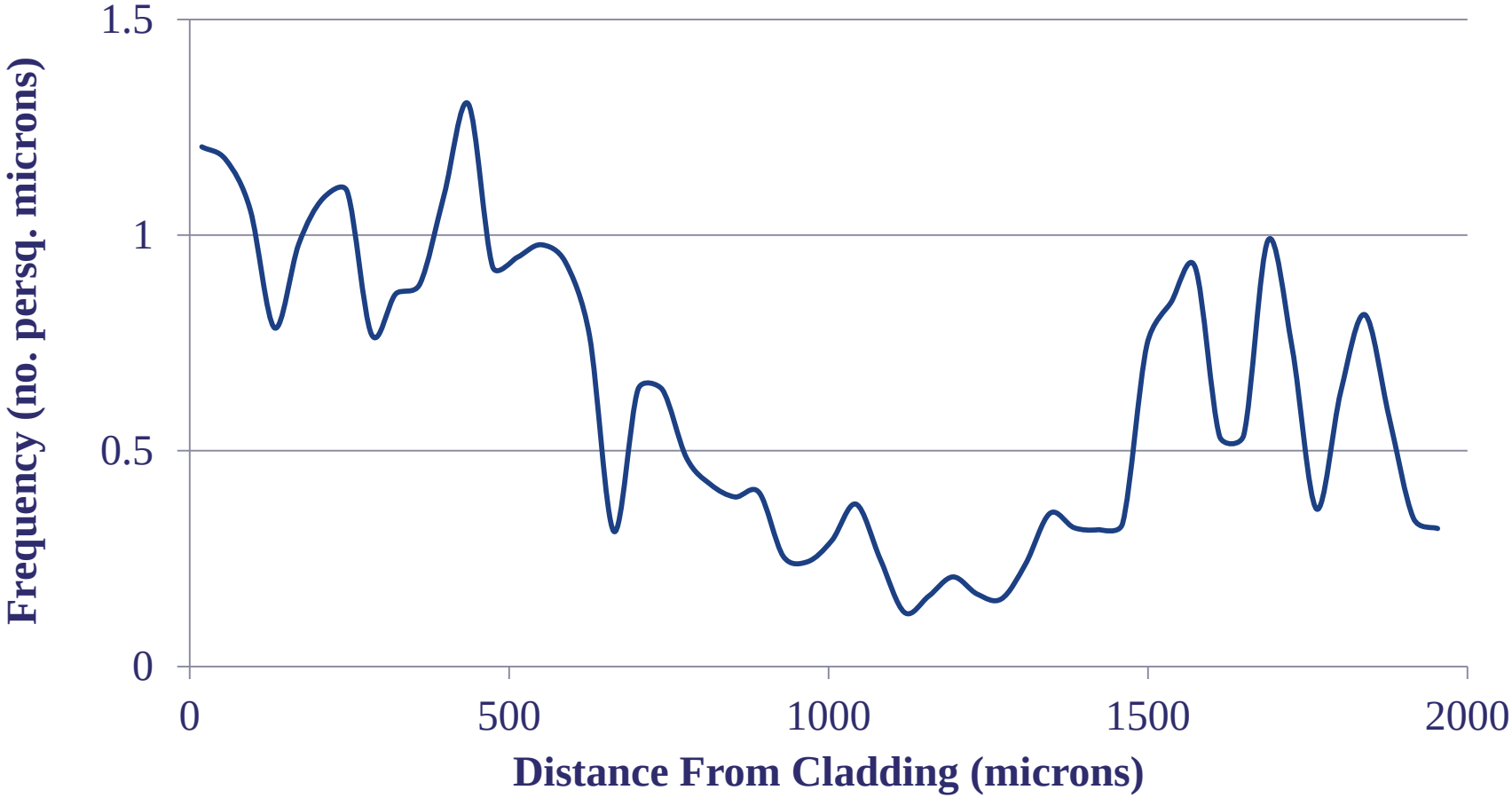
1.5
1
0.5
0
Frequency (no. persq. microns)
0
500
1000
1500
2000
Distance From Cladding (microns)

Fig. 3c

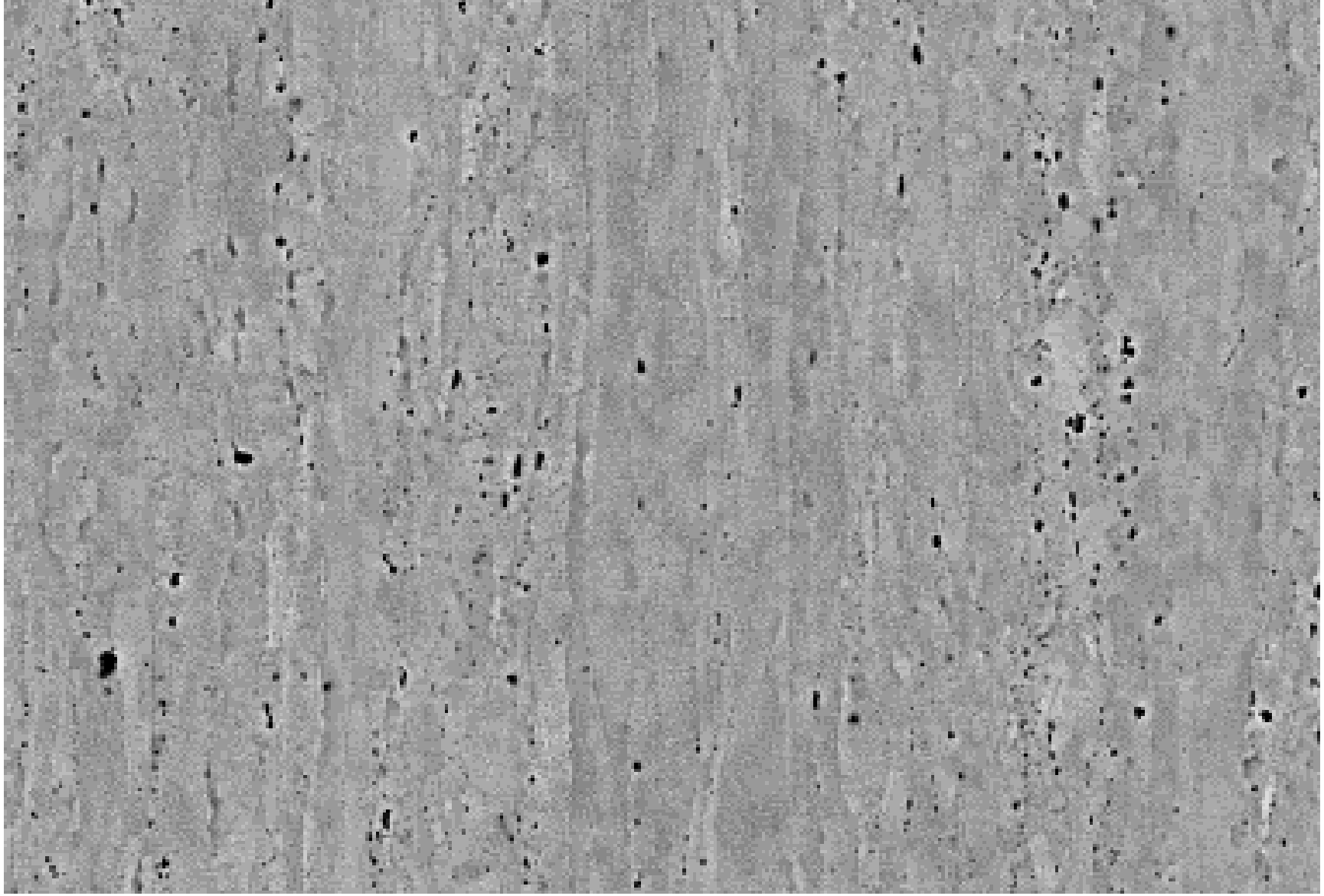

Fig. 3d . The micron bar is the same as in Fig. 3e. d. Cross-section SEM backscattered image showing alumina particle distribution in location A in Fig. 3a .

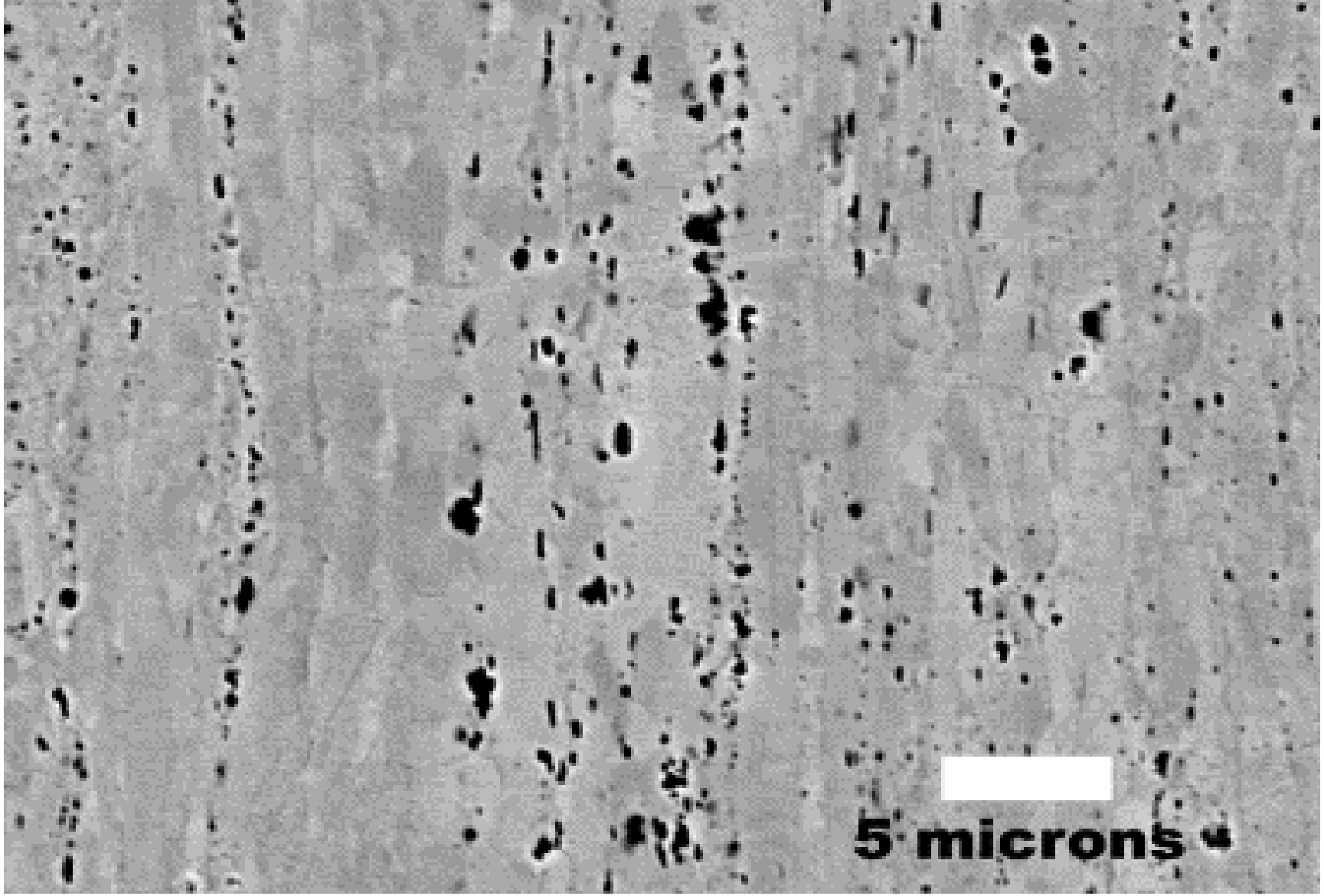

Fig. 3e. SEM backscattered image showing alumina particle distribution in location B in Fig. a.

Fig. 3. Particle distribution in longitudinal cross-section of an as-received GlidCop Al60 (particles greater than 80 nm were showed in Fig a. the scale bar in Fig.s c and d is the same): a. Particle size distribution in an area between 20 µm and 2000 µm away from the Cu cladding area; b. Particle volume fraction distribution in the same region as Fig. a; c. Particle frequency distribution in the same region as in Fig. a; d. Cross-section SEM backscattered image showing alumina particle distribution in location A in Fig. a; e. SEM backscattered image showing alumina particle distribution in location B in Fig. a. Images and data show that the size varies significantly, but the volume fraction remains similar in different regions.

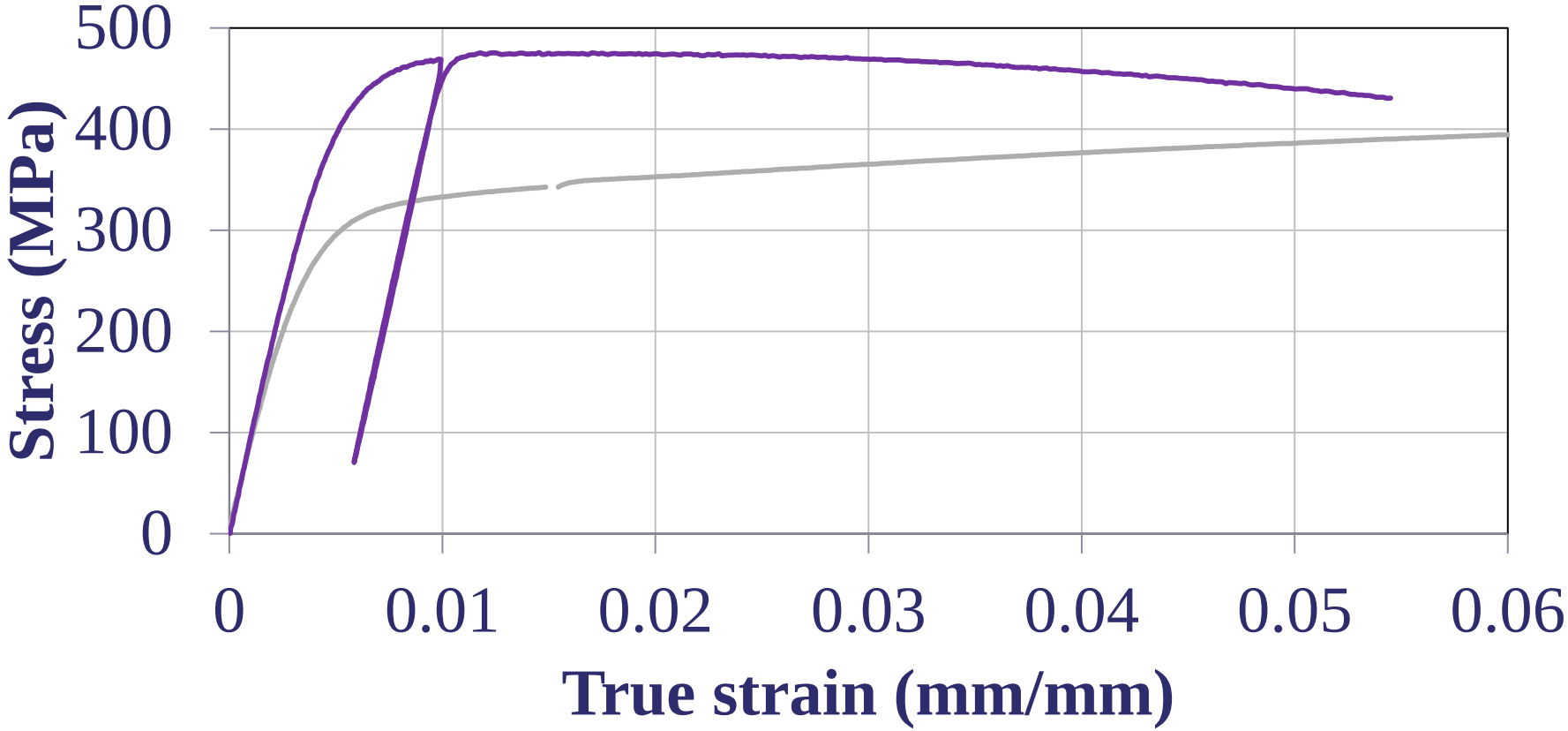

Fig. 4. Typical true stress-strain curves of as-received (thin orange line) and as-drawn samples. For as-drawn samples, the strain hardening rate, which is the slope of the stress-strain curves, becomes negative at strain of 2%. Strain- hardening rate remains positive at strain values greater than 15%.

TABLE II
PROPERTIES OF GLIDCOP AL60 AFTER DRAWING

	E (GPa)	YS (MPa)	TS (MPa)	ef (%)	RA (%)	Cond (%IACS)
RT Data *	111	524	565	7	42	82
No. of Tests	81	80	82	75	29	38
Stdev**	6	29	23	3	18	1
77 K Data	120	655	733	13	34	357
No of Tests	145	144	146	115	46	38
Stdev	7	37	29	3	16	13

*RT Data :Test conducted at room temperatures

**Stdev: Standard deviation of the tests

E: Elastic Young's modulus

YS: Yield Strength

TS: Tensile strength

ef: Elongation at fracture

RA: Reduction in Area at fracture

Con: Conductivity in International Annealed Copper Standard

Summary

Alumina particles in GlidCop conductors were examined by an FEG SEM. In images taken by backscattered electron detectors, small alumina particles show darker contrast than the matrix. In images taken by secondary electron or in-lens detector, however, these particles may show brighter contrast. Particles in size ranging from 5 nm to 5 μM, with most in nanometer scales, are distributed along the wire direction. The larger particles, which form a small volume fraction, are sparsely distributed in the matrix. Increasing alumina volume fraction and cold-deformation-strain enhances Young's modulus and mechanical strength. At 77 K, GlidCop conductors show higher values for Young's modulus, yield strength, tensile strength and elongation than at room temperatures. The reduction-in-area at fracture, however, remains the same. This indicates that overall ductility remains the same, but strain hardening rates are higher at 77 K, thus enhancing mechanical strength and homogeneous elongation.

ACKNOWLEDGMENT

We thank Dr. Tyler for editing the manuscript. We thank Dr. Chuck Mielke for helpful discussions. We thank NAH for supplying the GlidCop materials and Sam Dong in wire drawing. The work was undertaken in the National High Magnetic Field Laboratory, which is supported by NSF DMR-1157490, the State of Florida, and DOE.